JOURNAL OF VIROLOGY, Oct. 2011, p. 9929–9944 Vol. 85, No. 19
0022-538X/11/$12.00 doi:10.1128/JVI.05356-11

T Cells Are Not Required for Pathogenesis in the Syrian Hamster Model of Hantavirus Pulmonary Syndrome▽

Christopher D. Hammerbeck and Jay W. Hooper*

U.S. Army Medical Research Institute of Infectious Diseases, Virology Division, 1425 Porter Street, Fort Detrick, Maryland 21702

Received 9 June 2011/Accepted 7 July 2011

Andes virus (ANDV) is associated with a lethal vascular leak syndrome in humans termed hantavirus pulmonary syndrome (HPS). In hamsters, ANDV causes a respiratory distress syndrome closely resembling human HPS. The mechanism for the massive vascular leakage associated with HPS is poorly understood; however, T cell immunopathology has been implicated on the basis of circumstantial and corollary evidence. Here, we show that following ANDV challenge, hamster T cell activation corresponds with the onset of disease. However, treatment with cyclophosphamide or specific T cell depletion does not impact the course of disease or alter the number of surviving animals, despite significant reductions in T cell number. These data demonstrate, for the first time, that T cells are not required for hantavirus pathogenesis in the hamster model of human HPS. Depletion of T cells from Syrian hamsters did not significantly influence early events in disease progression. Moreover, these data argue for a mechanism of hantavirus-induced vascular permeability that does not involve T cell immunopathology.

Pathogenic hantaviruses represent a group of rodent-borne viruses of the *Bunyaviridae* family that cause hemorrhagic fever in humans (68). Infection of the rodent host results in a nonpathogenic persistent infection (16). In humans, though, infection causes two lethal vascular leak syndromes (36). Hemorrhagic fever with renal syndrome (HFRS), caused by Old World hantaviruses (e.g., Hantaan virus [HTNV] and Puumala virus [PUUV]) found throughout Europe and Asia, primarily affects the kidneys and has a case-fatality rate of ~5 to 15%. Hantavirus pulmonary syndrome (HPS), caused by New World hantaviruses (e.g., Sin Nombre virus [SNV] and Andes virus [ANDV]) found across the Americas, primarily affects the lungs and heart and has an overall mortality rate of ~40%, despite state-of-the-art treatment in modern intensive care facilities. Moreover, there is evidence that ANDV can be transmitted person to person (44, 77, 82). There are no FDA-licensed vaccines or therapies for these neglected diseases.

The mechanism underlying the vascular leakage caused by hantavirus infection is poorly understood. Hantaviruses primarily infect endothelial cells, but replication in these cells is not directly cytopathic (32, 33, 57, 83, 86, 88). Multiple mechanisms have been proposed to account for the vascular leakage caused by hantaviruses, including, predominantly, T cell-mediated immunopathology (4, 17, 39, 76, 79). Consistent with this, SNV-specific T cells induce permeability of human endothelial cells expressing SNV antigens *in vitro* (29). In humans, large numbers of T cells and cytokine-producing cells have been reported in the lungs, spleens, and hearts of HPS patients (52, 57, 88), and T cell numbers have been suggested to correlate with disease severity (39). During the acute phase of HFRS and in fatal HPS cases, cellular infiltrates have been reported to consist of disproportionately large numbers of activated $CD8^+$ T cells (33) (10, 54, 75). Genetic correlations between disease severity and HLA haplotype have been observed in patients with milder forms of HFRS and HPS, further implicating a role for T cell responses in pathogenesis (39, 47, 55, 56). These data have led some to suggest that therapeutically targeting T cells to improve the outcome of human infection could be an effective treatment option (76).

Despite this circumstantial evidence, efforts to directly test the role of T cells in hantavirus disease have been hampered by the absence of an animal model of hantavirus disease. Recently, we demonstrated that ANDV infection of adult Syrian hamsters (*Mesocricetus auratus*) causes a lethal vascular leak syndrome resembling clinical human HPS (32, 83). Here we used this model to investigate whether T cells contribute to hantavirus pathogenesis. Using this model, we found that while the accumulation of activated T cells in the lungs of hamsters correlated with disease onset and death, there was no difference in the kinetics or severity of disease when T cells were depleted with the chemotherapeutic agent cyclophosphamide (CyP) or T cell-specific antibodies. These data demonstrate, for the first time using a lethal adult animal model of human hantavirus disease, that T cells do not play a role in HPS.

MATERIALS AND METHODS

Virus and challenge of hamsters with virus. ANDV strain Chile-9717869 (32) was propagated in Vero E6 cells (Vero C1008; ATCC CRL 1586). Six- to 8-week-old female Syrian hamsters weighing 100 to 150 g (Harlan, Indianapolis, IN) were anesthetized by inhalation of vaporized isoflurane using an IMPAC 6 veterinary anesthesia machine. Once anesthetized, hamsters were injected with 2,000 PFU of virus diluted in sterile phosphate-buffered saline (PBS), pH 7.4. Intramuscular (i.m.) (caudal thigh) injections consisted of 0.2 ml delivered with a 1-ml syringe with a 25-gauge, 5/8-in. needle. Intranasal (i.n.) injections consisted of 50 μl delivered as 25 μl per naris with a plastic pipette tip.

Fluorescence-activated cell sorter (FACS) analysis. Blood was collected into EDTA-coated K2 Vacutainer tubes and gently inverted to mix. Animals were then euthanized and spleen and lung tissue was harvested into PBS. In experiments analyzing T cell kinetics, hamsters were perfused with sterile saline (Baxter) before spleen and lung tissue was removed. To isolate peripheral blood T

* Corresponding author. Mailing address: U.S. Army Medical Research Institute of Infectious Diseases, Virology Division, 1425 Porter Street, Fort Detrick, MD 21702. Phone: (301) 619-4101. Fax: (301) 619-2439. E-mail: jay.hooper@amedd.army.mil.

▽ Published ahead of print on 20 July 2011.

cells, EDTA-treated blood was transferred into Accuspin Histopaque columns (Sigma-Aldrich) and centrifuged at 1,000 × *g* for 10 min to remove red blood cells. Peripheral blood mononuclear cells were then isolated from the cell-serum interface and washed twice in PBS containing 2% fetal bovine serum (FBS). To isolate T cells from spleen and lung tissue, spleens and lungs were minced, incubated with collagenase D (Roche) for 20 min at 37°C, and then dissociated using either a BD Medimachine (BD Biosciences) or a gentleMACs dissociator (Miltenyi Biotec) according to the manufacturers' recommendations. The cell layer was then collected and washed twice in PBS containing 2% FBS. In some experiments, cells were incubated at 4°C for 15 min in a blocking buffer consisting of PBS containing 2% FBS, 2% normal rat serum (Sigma-Aldrich), and 2% normal mouse serum (Sigma-Aldrich), prior to staining with antibody. Approximately 10^6 cells were stained with anti-Syrian hamster immunoglobulin G (IgG; heavy plus light chains; 0.4 μg/ml; eBioscience) and/or anti-Syrian hamster immunoglobulin M (IgM; heavy plus light chains; 0.4 μg/ml; adsorbed to prevent cross-reactivity; Rockland Immunochemicals) and, to prevent cross-reactivity, with mouse anti-rat CD8β (clone 341; 0.8 μg/ml; eBioscience), rat anti-mouse CD4 (clone GK1.5; 0.4 μg/ml; eBioscience), and mouse anti-mouse/rat major histocompatibility complex class II (MHC II I-E^k; clone 14-4-4S; 0.04 μg/ml; eBioscience) for 15 to 20 min at 4°C. To determine annexin V expression on T cells, cells were further stained with an allophycocyanin (APC)-conjugated annexin V antibody kit (eBioscience), per the manufacturer's recommendation. Stained cells were then were fixed in Cytofix buffer (BD Biosciences) for 15 min at 4°C, before being analyzed on a FACSCalibur flow cytometer (BD Biosciences) using CellQuest software (BD Biosciences) or a FACSCanto II flow cytometer (BD Biosciences) using FACsDiva software (BD Biosciences). Data were analyzed using FlowJo software (Treestar).

***In vitro* stimulation of hamster lymphocytes.** A single-cell suspension of peripheral blood, spleen, and lymph node cells was prepared as described. Cells were cultured in RPMI 1640 medium with 10% FCS, 4 mM L-glutamine, 0.1 mM nonessential amino acids, 1 mM sodium pyruvate, 100 U/ml penicillin and streptomycin, 10 mM HEPES, and 5×10^{-6} M 2-mercaptoethanol (RP-10). Bulk lymphocytes were then placed in microtiter wells (5×10^5 per well) containing 40 ng/ml lipopolysaccharide (LPS; *Escherichia coli*; L6529; Sigma-Aldrich) or 1 μg/ml concanavalin A (ConA; catalog no. 234567; Calbiochem) and were incubated at 37°C for the indicated amount of time. In some experiments, cells were labeled with carboxyfluorescein succinimidyl ester (CFSE; Molecular Probes).

***In vivo* BrdU labeling.** Hamsters were given sterile drinking water containing 0.8 mg/ml bromodeoxyuridine (BrdU; Sigma-Aldrich) beginning 3 days before ANDV challenge. Water containing BrdU was then given continuously and was changed every 1 to 2 days. Intracellular staining for BrdU was done using an APC BrdU flow kit (BD Biosciences) according to the manufacturer's recommendations.

***In vivo* cyclophosphamide administration.** Cyclophosphamide monohydrate was purchased from Sigma-Aldrich. On the indicated days, anesthetized hamsters were injected intraperitoneally (i.p.) with 100 mg/kg of body weight cyclophosphamide monohydrate diluted in sterile PBS, pH 7.4.

***In vivo* T cell depletion.** Functional-grade mouse anti-rat CD8β antibody (clone 341) was purchased from eBioscience. All other antibodies used in the *in vivo* depletion experiments were purified from hybridomas. The hybridoma for rat anti-mouse CD4 (clone GK1.5) was purchased from ATCC (CRL TIB-207). The hybridoma for rat IgG2b was a gift from John Kearny. The hybridoma for mouse IgG1 was obtained in-house and secretes an antibody to an irrelevant vaccinia virus epitope. Anesthetized hamsters were injected with combinations of purified rat anti-mouse CD4 or rat IgG1 isotype control antibodies (2 mg intraperitoneally in 1.0 ml) and mouse anti-rat CD8β or mouse IgG2b isotype control antibodies (1 mg intraperitoneally in 0.5 ml) diluted in sterile PBS, pH 7.4.

Preparation of tissue for histology. Tissues were fixed in 10% neutral-buffered formalin, trimmed, processed, embedded in paraffin, cut at 5 to 6 μm, and stained with hematoxylin-eosin (H&E). Immunolocalization of ANDV in tissues was performed with an immunoperoxidase procedure (horseradish peroxidase EnVision system; Dako) according to the manufacturer's directions. The primary antibody was an anti-SNV nucleocapsid rabbit polyclonal antibody diluted 1:3,000 (provided by Diagnostic Service Division, USAMRIID). Negative controls included naïve hamster tissue incubated with nonimmune rabbit IgG in place of the primary antibody and naïve hamster tissue exposed to the primary antibody and to negative serum. After deparaffinization and peroxidase blocking, tissue sections were pretreated with proteinase K for 6 min at room temperature, rinsed, and then covered with primary antibody and incubated at room temperature for 1 h. They were rinsed, and then the peroxidase-labeled polymer (secondary antibody) was applied for 30 min. Slides were rinsed, and a substrate-chromogen solution (3,3′-diaminobenzidine; Dako) was applied for 5 min. The substrate-chromogen solution was rinsed off the slides, and the slides were stained with hematoxylin and rinsed. The sections were dehydrated and cleared with xyless, and then a coverslip was placed.

Statistical analyses. Data are means ± standard deviations (SDs). We used the Kaplan-Meier log-rank survival test or Student's *t* test, as indicated. We considered all *P* values of >0.05 to be insignificant.

Ethics statement. All work involving the use of ANDV in animals was performed in USAMRIID's biosafety level 4 laboratory. The hamster research protocol was approved by the U.S. Army Medical Research Institute of Infectious Disease Institutional Animal Care and Use Committee (USDA registration number 51-F-0021; PHS assurance number A3473-01), in compliance with the Animal Welfare Act and other federal statutes and regulations relating to animals and experiments involving animals, and adhered to the principles stated in the *Guide for the Care and Use of Laboratory Animals* (56a). The facility where this research was conducted is fully accredited by the Association for Assessment and Accreditation of Laboratory Animal Care International.

RESULTS

Kinetics of T cell activation in ANDV-infected hamsters. Activated T cells are known to be present at sites of human hantavirus infection (52, 57, 88), but little is known about the T cell response to hantavirus infection in hamsters. In order to identify T cells in hamsters, commercially available antibodies were screened for cross-reactivity in the hamster model (Table 1). Three of these antibodies uniquely identified populations of B cells, $CD4^+$ T cells, and $CD8^+$ T cells in hamsters (Fig. 1A and Table 2). While anti-mouse/rat I-E^k (clone 14-4-4S) and anti-mouse CD4 (clone GK1.5) have previously been demonstrated to identify hamster B cells (45) and $CD4^+$ T cells (14), respectively, we found that anti-rat CD8β (clone 341) labeled a third cell population, presumably hamster $CD8^+$ T cells, that was found to be both I-E^k and CD4 negative and proliferated in response to ConA (Fig. 1C). Neither the $CD4^+$ nor $CD8\beta^+$ population bound the I-E^k antibody, indicating that labeling of cells with these three antibodies was mutually exclusive (Fig. 1B), and only cells bound by the I-E^k antibody were found to express immunoglobulins M and G (Fig. 1A). Interestingly, when injected into hamsters intraperitoneally, the mouse CD4 and rat CD8β antibodies were found to deplete their respective T cell subsets in both lymphoid and nonlymphoid tissues compared to animals receiving relevant mouse and rat isotype control antibodies (Fig. 1D). Importantly, the reduction in T cells correlated with a reduction in the percentage of MHC II-negative (MHC II^-)/immunoglobulin-negative (IgG^-) cells (Fig. 1E) in each tissue type, demonstrating that the CD4 and CD8β antibodies were, in fact, capable of depleting their respective T cell subsets.

To determine if the kinetics of the hamster T cell response to ANDV infection coincided with disease onset, hamsters were challenged with ANDV i.m., and then peripheral blood, spleen tissue, and lung tissue were analyzed every 3 days through day 12 (Fig. 2A). Using BrdU incorporation as an indicator of proliferation, 10% of the $CD4^+$ T cells were BrdU ($BrdU^+$) positive in the lung on the day of ANDV challenge, and this percentage remained unchanged through day 6 (Fig. 2C and D). Between day 6 and day 9, however, the percentage of $BrdU^+$ $CD4^+$ T cells increased from 10% to 19%, consistent with an increase in total $CD4^+$ T cells in the lung during this time (Fig. 2B). The percentage of $BrdU^+$ $CD8^+$ T cells in the lung progressively increased across all time points but also peaked on day 9 (16%), similar to the increase in the total numbers of $CD8^+$ T cells (Fig. 2B). In the spleen, approxi-

TABLE 1. Antibodies screened for cross-reactivity in the Syrian hamster

Antigen	Host species	Reactivity	Clone	Isotype	Cross-reactivity
MHC II (I-E^k)	Mouse	Mouse/rat	14-4-4s	IgG2a	++++
CD3	Mouse	Rat	G4.18	IgG3	−
	Mouse	Rat	IF4	IgM	−
	Mouse	Human	HIT3	IgG2a	−
	Mouse	Human	UCHT1	IgG1	−
	Mouse	Human	OKT3	IgG2a	−
	Mouse	NHP[a]	SP34-2	IgG1	−
	Rat	Mouse	17A2	IgG2b	−
	Arm. hamster[b]	Mouse	145-2C11	IgG	−
	Rat	Mouse	KT3	IgG2a	−
CD4	Mouse	Rat	OX-38	IgG2a	−
	Mouse	Human	RPA-T4	IgG1	−
	Rat	Mouse	GK1.5	IgG2b	++++
CD8α	Mouse	Rat	G28	IgG2a	−
	Mouse	Rat	OX-8	IgG1	−
	Mouse	Human	HITa	IgG1	−
	Mouse	Human	OKT8	IgG2a	−
	Mouse	Human	RPA-T8	IgG1	−
	Rat	Mouse	KT15	IgG2a	−
	Rat	Mouse	5H10-1	IgG2b	−
CD8β	Mouse	Rat	341	IgG1	+++
	Rat	Mouse	CT-CD8b	IgG2a	−
	Rat	Mouse	H35-17.2	IgG2b	−
	Rat	Mouse	53-5.8	IgG1	−
CD9	Mouse	Rabbit	MM2/57	IgG2b	−
CD25	Mouse	Rat	OX-39	IgG1	−
	Rat	Mouse	PC61.5	IgG1	−
CD27	Mouse	Human	O323	IgG1	−
	Arm. hamster	Mouse	LG.7FG	IgG	−
CD44	Mouse	Rat	OX-49	IgG2a	−
	Rat	Mouse	IM7	IgG2b	−
CD45R	Mouse	Rat	HIS24	IgG2b	−
	Rat	Mouse	RA3-6B2	IgG2a	−
CD45RA	Mouse	Rat	OX-33	IgG1	−
	Mouse	Human	H100	IgG2b	−
	Mouse	Human	JS-83	IgG	−
CD45RB	Mouse	Human	MEM-55	IgG1	−
	Rat	Mouse	C363.16A	IgG2a	−
CD45RC	Mouse	Rat	OX-22	IgG1	−
	Rat	Mouse	GL24	IgM	−
CD45RO	Mouse	Human	UCHL1	IgG2a	−
CD57	Mouse	Human	NK-1	IgM	−
CD62L	Mouse	Rat	OX-85	IgG1	−
	Arm. hamster	Rat	HRL1	IgG2	−
	Mouse	Human	Dreg-56	IgG1	−
	Rat	Mouse	MEL-14	IgG2a	−
CD79a	Mouse	Human	HM57	IgG1	−
Thy1.1	Rat	Mouse	OX-7	IgG1	−
Thy1.2	Mouse	Rat	T1-H7	IgM	−
	Rat	Mouse	53-2.1	IgG2a	−
	Mouse	Mouse	HO-13-4[c]	IgM	++++
	Rat	Mouse	30-H12	IgG2b	−

[a] NHP, nonhuman primate.
[b] Arm. hamster, Armenian hamster.
[c] Not unique; it labeled all hamster lymphocytes tested.

mately 7% of CD4$^+$ T cells and 3% of CD8$^+$ T cells were found to be BrdU$^+$ on day 0 (Fig. 2D and data not shown). As with total CD4$^+$ T cell number (Fig. 2B), the percentage of BrdU$^+$ CD4$^+$ T cells decreased slightly by day 3 and then steadily increased to approximately 18% of total CD4$^+$ T cells by day 9. By comparison, the percentage of BrdU$^+$ CD8$^+$ T cells increased only gradually by day 6 (from 3% to 5%) but increased more significantly to approximately 13% by day 9 (Fig. 2D and data not shown), while total CD8$^+$ cells increased steadily between days 3 and 9 (Fig. 2B). The decrease in CD4$^+$ T cell number and variability in CD8$^+$ T cell number early after infection correlated with an increased amount of apoptosis of T cells in the spleen, as measured by annexin V (Fig. 2E). No decrease was observed in CD4$^+$ T cell number in the lung, even though we detected an increase in CD4$^+$ T cell apoptosis (Fig. 2E). The increase in annexin V staining in the lung was specific to the CD4$^+$ T cell compartment, as no increase in annexin V was seen on CD8$^+$ T cells (Fig. 2E). Notably, total CD4$^+$ and CD8$^+$ T cell numbers in both the spleen and lung decreased to preinfection (day 0) levels between day 9 and day 12 (Fig. 2B), which was concomitant with the onset of disease and death of infected animals (Fig. 2A). Annexin V staining of CD4$^+$ T cells in the lung and spleen remained slightly elevated between day 3 and day 9, but the percentage of annexin V-positive cells did not exceed the levels found on day 3 (data not shown). Similarly, annexin V staining of CD8$^+$ T cells in the spleen remained slightly elevated between day 3 and day 9, yet the percentage of annexin V-positive CD8$^+$ T cells in the lung remained largely unchanged from the levels found on day 0 or 3 (data not shown). The percentage of BrdU-positive T cells did not increase but remained largely unchanged or decreased slightly. This suggested that the T cell populations that remained in the lung and spleen on day 12 were not enriched for effector cells. Taken together, these data suggest that the peak accumulation of activated, BrdU$^+$ T cells in the lung and spleen 9 days after virus challenge correlates with the death of infected hamsters beginning a day later.

Cyclophosphamide fails to alter disease following intramuscular ANDV challenge. We hypothesized that if T cells were involved in the pathogenesis of hantavirus disease, then depletion of T cells would alter the kinetics of and possibly ameliorate disease in hamsters. CyP is a well-known chemotherapeutic agent and alkylating cytotoxic drug that affects T cells, B cells, and other proliferating cells (7). Therefore, we used CyP to deplete T cells during ANDV infection. Hamsters were challenged i.m. with ANDV and then treated with CyP or PBS i.p. at 6, 7, and 8 days postchallenge, consistent with the timing of T cell activation shown in Fig. 2. Total leukocyte numbers in the blood and spleens of ANDV-challenged animals were significantly reduced on day 9 by CyP treatment compared to PBS treatment (Fig. 3A). In the absence of infection, leukocyte numbers in the lung were also reduced by CyP, but not significantly, compared to PBS control animals. CD4$^+$ and CD8$^+$ T cell numbers were significantly reduced in the spleen (50 to 60%) and lungs and peripheral blood (80 to 85%) of ANDV-challenged animals following CyP treatment (Fig. 3B), and B cell numbers were reduced by nearly 90% in all tissues examined (Fig. 3C). Despite reduced T and B cell numbers, there was no significant difference in the mean time to death of animals receiving CyP (11 days) and those receiving PBS (11.45 days) (Fig. 3D). These results demonstrate that CyP does not alter the course of hantavirus disease, despite reducing T and B cell numbers.

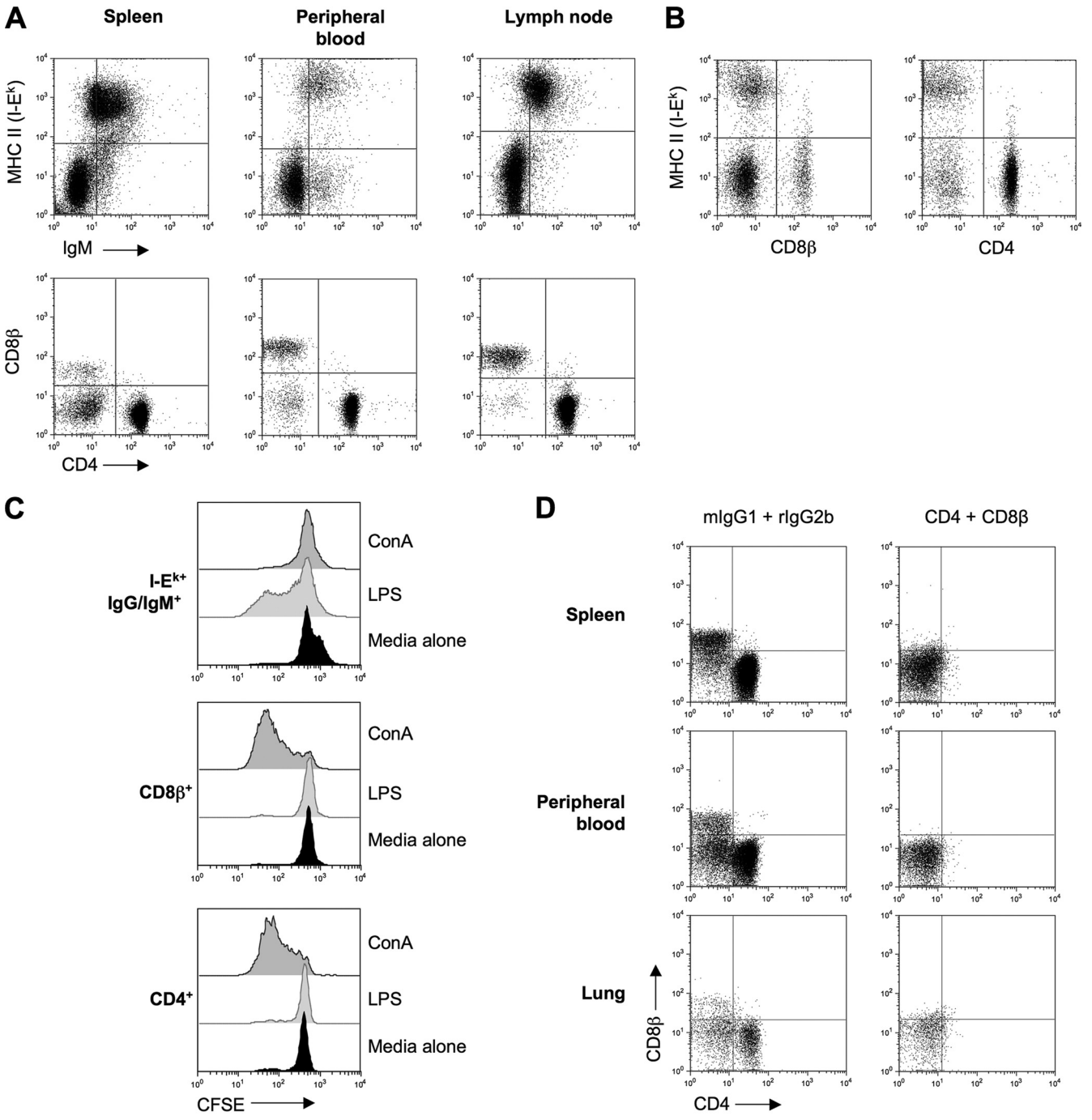
A
Spleen
Peripheral blood
Lymph node
MHC II (I-E^k)
IgM
CD8β
CD4
B
MHC II (I-E^k)
CD8β
CD4
C
I-E^k+ IgG/IgM+
ConA
LPS
Media alone
CD8β+
ConA
LPS
Media alone
CD4+
ConA
LPS
Media alone
CFSE
D
mIgG1 + rIgG2b
CD4 + CD8β
Spleen
Peripheral blood
Lung
CD8β
CD4

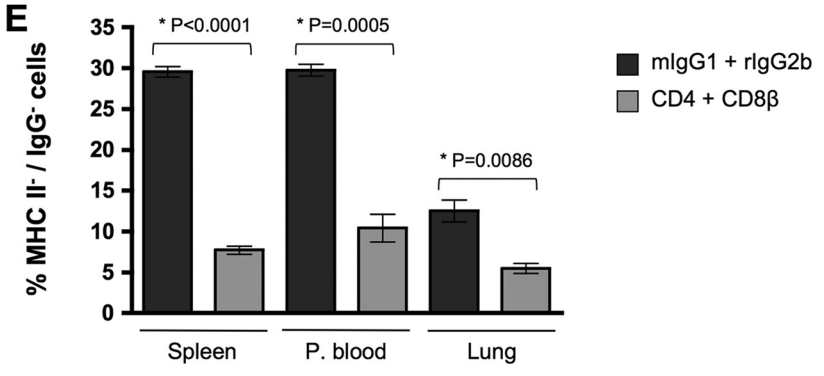
E
% MHC II- / IgG- cells
* P<0.0001
* P=0.0005
* P=0.0086
mIgG1 + rIgG2b
CD4 + CD8β
Spleen
P. blood
Lung

TABLE 2. Distribution of T and B cell subsets in peripheral blood and secondary lymphoid tissue

Specimen	Population	% of total lymphocytes	Distribution of $CD4^+$ and $CD8\beta^+$ subsets (% of $I\text{-}E^{k-}$ lymphocytes)	Distribution of IgG^+/IgM^+ subsets (% of $I\text{-}E^{k+}$ lymphocytes)
Peripheral blood	$I\text{-}E^{k+}/(IgG/IgM^+)$	14.5 ± 2.0		80.4 ± 7.6
	$CD4^+$	58.3 ± 3.7	74.5 ± 4.4	
	$CD8\beta^+$	12.4 ± 2.6	14.3 ± 3.5	
Lymph node	$I\text{-}E^{k+}/(IgG/IgM^+)$	31.3 ± 2.5		92.0 ± 0.8
	$CD4^+$	51.4 ± 4.1	76.9 ± 5.1	
	$CD8\beta^+$	13.9 ± 3.3	19.7 ± 4.9	
Spleen	$I\text{-}E^{k+}/(IgG/IgM^+)$	45.8 ± 6.8		92.0 ± 4.7
	$CD4^+$	39.9 ± 12.3	69.9 ± 19.4	
	$CD8\beta^+$	2.6 ± 1.5	4.0 ± 2.9	

Cyclophosphamide fails to alter disease following intranasal ANDV challenge. Transmission of hantavirus to humans is thought to be due to inhalation of aerosolized rodent excreta. We were therefore interested in determining whether cyclophosphamide would be any more effective in protecting hamsters following intranasal ANDV challenge. Hamsters were challenged i.n. with ANDV and were then treated with CyP or an equivalent amount of PBS (i.p.) at 8 and 11 days postchallenge. Hamsters challenged with ANDV developed disease and died whether they received PBS or CyP. No significant differences were found in the time to death of CyP-treated animals compared to PBS-treated animals (Fig. 4A). One CyP-treated animal died on day 25 from a cause unrelated to CyP therapy. The lack of effect of CyP on survival was not due to a failure to deplete T cells, though, because we found that on day 14 the numbers of leukocytes (Fig. 4B) and $CD4^+$ and $CD8^+$ T cells (Fig. 4C) in the spleen were reduced by approximately 63% compared to PBS controls. The observation that T cell numbers were not significantly increased in ANDV-challenged hamsters compared to unchallenged hamsters suggested that the T cell response to i.n. ANDV challenge may begin after day 14 and that administration of CyP on day 8 and day 11 may not effectively deplete effector T cells. To address this, we performed a second experiment in which we challenged hamsters with ANDV but varied the times that CyP was administered. There were no significant differences between the mean times to death of the animals receiving PBS and animals in the groups receiving CyP on days 8, 11, and 14; days 11 and 14; or days 11, 14, and 17 (Fig. 4D). One hamster receiving PBS did survive. These results demonstrated that reduced T cell numbers following intranasal or intramuscular ANDV challenge did not have any detectable effect on the progression or outcome of hantavirus disease.

Depletion of Syrian hamster T cells fails to alter pathogenesis. CyP can deplete multiple cell types, including T and B cells (7) (Fig. 3 and 4). To specifically determine the role of T cells in pathogenesis, hamsters were challenged with ANDV, and then T cells were depleted by administering combinations of anti-CD4 or anti-CD8β antibodies or the relevant isotype control antibodies, as demonstrated in Fig. 1, at 6 and 8 days postchallenge. To confirm depletion, blood and lung tissue were analyzed by flow cytometry on day 9 (Fig. 5A). There was a 49-fold reduction (0.78% versus 38%) in the percentage of $CD4^+$ T cells in the blood of hamsters receiving the CD4 antibody compared to hamsters treated with an isotype-matched rat control antibody (Fig. 5B). Similarly, there was a 39-fold reduction in the percentage of $CD8^+$ T cells in hamsters receiving the CD8β antibody compared to hamsters treated with an isotype-matched mouse control antibody (0.19% versus 7.5%) (Fig. 5C). Similar results were also obtained when hamsters received a combination of CD4 and CD8β antibodies or isotype-matched control antibodies (Fig. 5D). A reduction in the percentage of CD4 and CD8 T cells was also observed in the lungs of animals treated with CD4 and CD8 antibodies, either alone (Fig. 5B and C, respectively) or in combination (Fig. 5D), compared to animals treated with isotype control antibodies. Despite this, no significant difference was observed in the number of surviving animals or the mean time to death of animals treated with CD4 or CD8β antibodies alone (Fig. 5E and F, respectively) or in combination (Fig. 5G) compared to animals treated with isotype control antibodies or PBS. Taken together, these

FIG. 1. Identification of T cell subsets in Syrian hamsters. Cells from peripheral blood, lymph node, and spleen of normal hamsters were stained with antibodies as described in Materials and Methods and analyzed by flow cytometry to identify hamster T cell subsets. (A) The $I\text{-}E^k$ and IgM staining profiles of cells were based on bulk live cells. CD4 and CD8β staining was based on $I\text{-}E^k$-negative ($I\text{-}E^{k-}$)/IgM^- cells. (B) To ensure that $CD4^+$ and $CD8\beta^+$ cells were uniquely $I\text{-}E^{k-}$, bulk live cells ($I\text{-}E^{k-}$ and $I\text{-}E^k$-positive [$I\text{-}E^{k+}$]) were analyzed for binding of the $I\text{-}E^k$ antibody. Results for lymph node cells are shown. Identical results were also found in the spleen and peripheral blood. All gates were determined by using a relevant nonbinding isotype control antibody. The percentage of cells that stained positive with the relevant isotype control antibodies was less than 0.1% for all antibodies. Results are representative of five independent experiments. (C) Hamster lymphocytes were CFSE labeled and then stimulated for 72 h in the presence of medium alone, LPS, or ConA to test their ability to proliferate in response to either B or T cell mitogens. CFSE dye dilution at 72 h was determined for each cell subset by flow cytometry. To determine if antibodies could deplete T cells *in vivo*, hamsters were given anti-CD4 and anti-CD8β antibodies or relevant isotype control antibodies i.p. on day 0 and day 2. Spleen, peripheral blood, and lung tissue were analyzed by flow cytometry on day 3 to determine the presence or absence of $CD4^+$ and $CD8^+$ subsets ($n = 3$) (D) and the percentage of $I\text{-}E^{k-}/IgM^-$ cells (E). mIgG1, mouse IgG1; rIgG2b, rat IgG2b. Results are representative of two independent experiments.

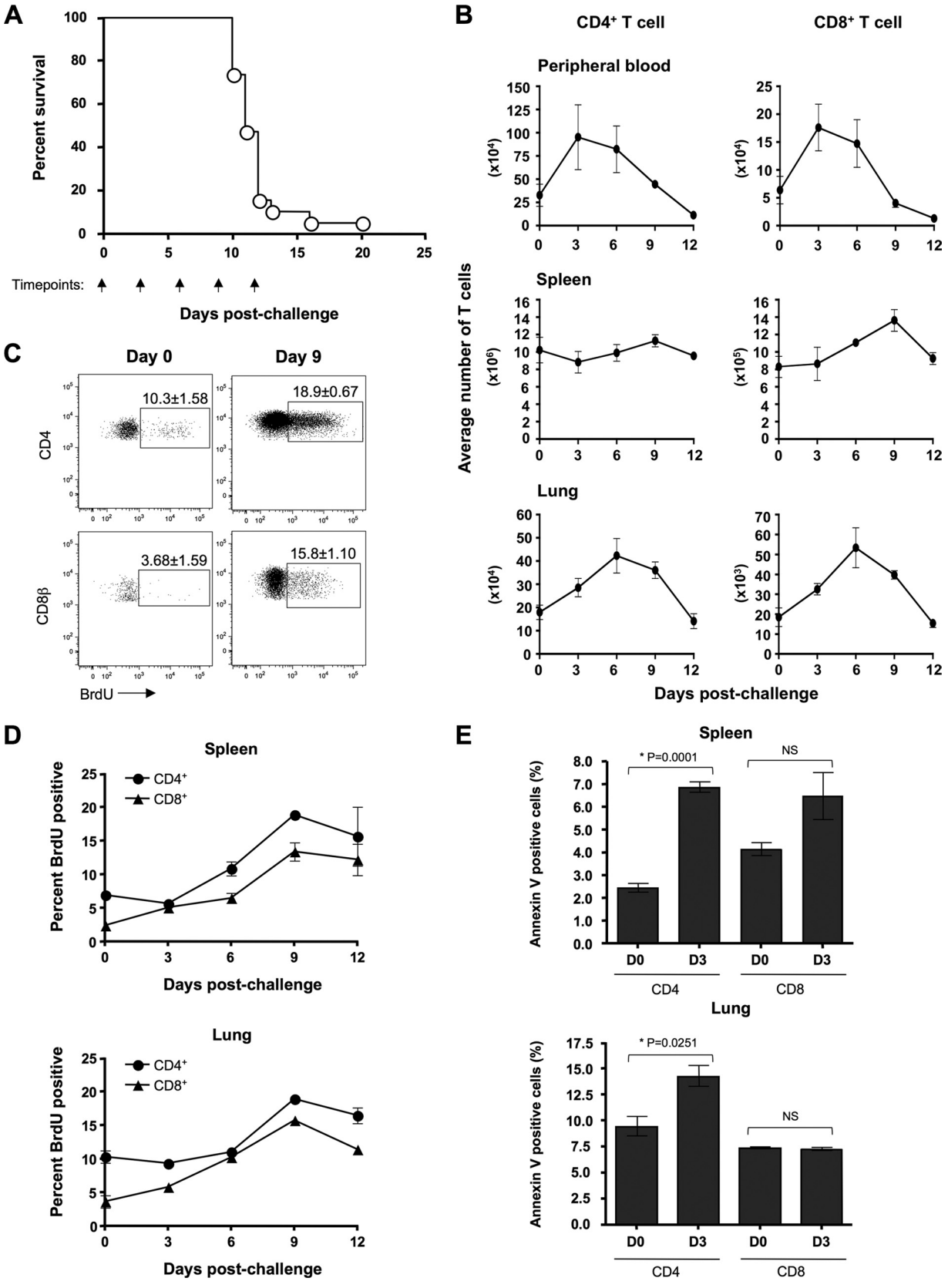
A
Percent survival
Timepoints:
Days post-challenge
B
CD4+ T cell
CD8+ T cell
Peripheral blood
Spleen
Lung
Average number of T cells
Days post-challenge
C
Day 0
Day 9
10.3±1.58
18.9±0.67
3.68±1.59
15.8±1.10
CD4
CD8β
BrdU
D
Spleen
Lung
Percent BrdU positive
CD4+
CD8+
Days post-challenge
E
Spleen
Lung
Annexin V positive cells (%)
* P=0.0001
NS
* P=0.0251
D0
D3
CD4
CD8

results confirm our CyP data and indicate that T cells are not involved in the pathogenesis of HPS.

Depletion of immune cells does not alter ANDV pathology. To ensure that disease pathogenesis following depletion of activated lymphocytes by CyP treatment was consistent with ANDV pathogenesis, histomorphologic analysis was performed on lung tissue from PBS-, CyP-, or antibody-treated animals infected with ANDV (Fig. 6A). Following both PBS and CyP treatments, lungs of ANDV-infected hamsters exhibited signs of subacute interstitial pneumonia consistent with ANDV infection. Interstitial inflammation was diffuse and moderate within the lungs of PBS-treated animals, while it was slightly milder following CyP treatment. Also present were scattered necrotic/apoptotic-like cellular debris evidence of fibrin deposition within the alveoli and signs of alveolar edema. Similarly, hamsters treated with either anti-CD4 or anti-CD8β antibodies or relevant isotype control antibodies also exhibited signs of subacute interstitial pneumonia, diffuse and moderate to marked interstitial inflammation, alveolar fibrin deposition, and edema characteristic of ANDV infection. Immunohistochemistry analysis of lung tissue from these groups further revealed multifocal granular cytoplasmic staining of cells for hantavirus antigen in the alveolar septa (most likely associated with endothelial cells of capillaries), endothelial cells in larger vessels, and scattered alveolar histiocytes (Fig. 6B). Immunohistochemistry analysis also suggested that there was little to no difference in overall viral load within endothelial cells following PBS, CyP, or antibody treatment. This suggests that the depletion of various immune cell types by CyP or antibody did not alter the pathology characteristic to ANDV infection.

Viral challenge dose and timing of T cell depletion do not alter pathogenesis. The disease progression in hamsters challenged with 2,000 PFU ANDV is highly uniform, making it a useful model for studying hantavirus disease. However, it was possible that any effect of T cell depletion was overwhelmed by the effects of 2,000 PFU of virus. Moreover, the accumulation of T cells in the lungs at 6 days postchallenge (Fig. 2) suggested the possibility that within these cells was a population of activated, yet undivided, cells capable of mediating disease before being depleted by antibody. To test these possibilities, a cohort of hamsters was first challenged with 80 PFU ANDV i.m. and disease progression was determined (Fig. 7A). The kinetics of disease following a low-dose 80-PFU challenge (mean time to death, 11.9 days) were similar to the disease kinetics following the 2,000-PFU challenge (Fig. 2), suggesting that T cell kinetics might also be similar. To then determine if the challenge dose and the timing of CyP or T cell-depleting antibody treatment affected the kinetics of disease, one group of hamsters was challenged intramuscularly with 80 PFU ANDV. These animals were then treated with CyP, PBS, combinations of anti-CD4 and anti-CD8β antibodies, or matched isotype control antibodies (i.p.) on days 4.5, 6, and 8 postchallenge. A second group of hamsters was challenged intramuscularly with 2,000 PFU ANDV and received the same treatments on days 4.5, 6, and 8 postchallenge. Even when administered earlier, CyP did not alter the course of disease following the 2,000-PFU ANDV challenge or following a low-dose 80-PFU ANDV challenge (Fig. 7B). Similarly, we still found no significant difference in the number of surviving animals or the mean time to death of animals treated with CD4 and CD8β antibodies (10.1 days) compared to animals treated with isotype control antibodies (10.2 days) or PBS (10.1 days) following the 2,000-PFU ANDV challenge or challenge with 80 PFU ANDV (CD4 and CD8β antibodies, 11.4 days; isotype control antibodies, 11.8 days; PBS, 10.8 days) (Fig. 7B). Thus, these data support our initial experiments and demonstrate that T cells are not required for hantavirus pathogenesis following low- or high-dose ANDV challenge.

DISCUSSION

Much of our knowledge regarding the relationship between T cells and hantavirus disease pathogenesis has been gleaned through indirect observation of tissue samples from humans infected by hantavirus and inferred by comparisons with diseases caused by other viruses in which pathogenesis is mediated by T cells. However, using the ANDV/Syrian hamster lethal disease model, we have now demonstrated directly that T cells are not required for HPS pathogenesis.

The role of T cells during viral infection can be paradoxical, in that while they may be necessary for protection, they can also contribute to pathology. During respiratory syncytial virus (RSV) infection in mice, $CD4^+$ and $CD8^+$ T cells contribute to virus clearance, but clearance results in significant lung pathology mediated by both T cell subsets (58, 80). Similarly, $CD8^+$ T cells have been linked with protection in mouse models of primary dengue virus infection, while memory T cells contribute to dengue hemorrhagic fever upon secondary dengue virus infection (65). In cases where T cell responses are protective, depletion of T cells can result in greater pathology and a decrease in time to death (70, 72). Conversely, when T cells are pathogenic, depletion often leads to decreased mortality (2, 18,

FIG. 2. Kinetics of the T cell response to ANDV in Syrian hamsters. Forty hamsters were challenged intramuscularly with 2,000 PFU of ANDV on day 0. Five hamsters were not challenged and were used for day 0 analyses. (A) Schematic representation depicting the number of days that T cell numbers were determined in relation to the survival of ANDV-challenged hamsters. On the day of challenge and then every 3 days thereafter, five hamsters each were euthanized and peripheral blood, spleen tissue, and lung tissue were harvested to determine T cell numbers ($n = 5$). All animals euthanized on day 12 were displaying signs and symptoms of disease. A separate group of animals was challenged with ANDV and then monitored for survival ($n = 12$). On the indicated days (arrows), five hamsters each were euthanized and peripheral blood, spleen tissue, and lung tissue were harvested to determine the numbers of $CD4^+$ and $CD8^+$ T cells in each tissue at each time point during ANDV infection (B). (C) To determine when T cell activation occurs following ANDV infection, spleen and lung cells were stained for BrdU and analyzed by flow cytometry (data for day 0 and day 9 are shown; data for spleen cells are not shown). Values are means ± SDs. (D) The percentages of $BrdU^+$ $CD4^+$ and $CD8^+$ T cells in the spleen and the lung were then determined at the indicated times after infection. (E) To determine if T cells undergo apoptosis early after ANDV challenge, the percentage of annexin V-positive cells in the spleen and lung was determined. The *P* value was determined by unpaired two-tailed Student's *t* test. D0 and D3, days 0 and 3, respectively; NS, not significant. Values are means ± SDs. Results are representative of two independent experiments.

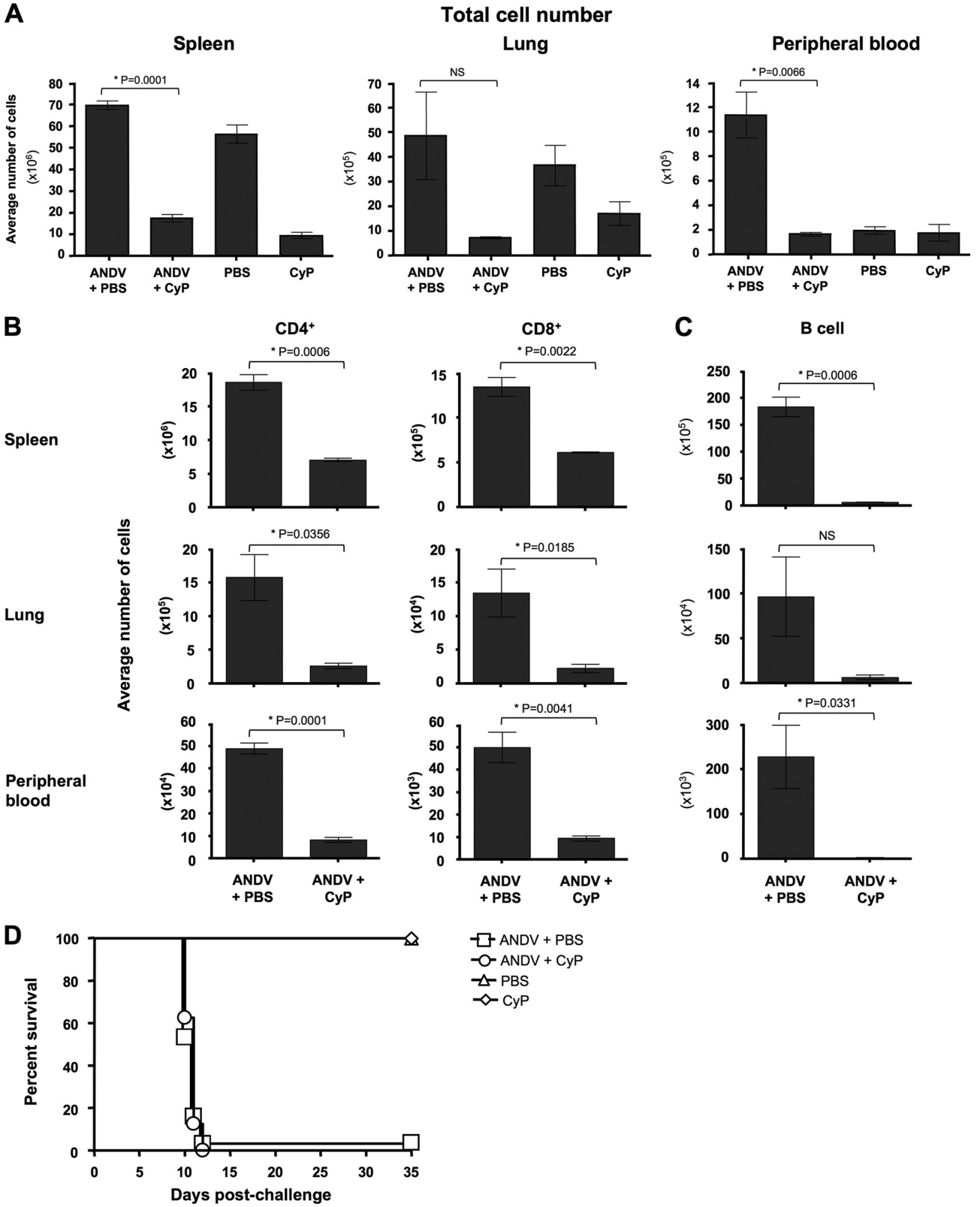

FIG. 3. Cyclophosphamide does not alter disease pathogenesis following intramuscular ANDV challenge. Hamsters were challenged intramuscularly with 2,000 PFU of ANDV. At 6, 7, and 8 days after challenge, hamsters challenged with ANDV were given 100 mg/kg cyclophosphamide intraperitoneally (ANDV + CyP) or an equivalent amount of PBS (ANDV + PBS). Two control groups of hamsters that were not challenged with ANDV were given 100 mg/kg CyP or an equivalent amount of PBS. The effect of cyclophosphamide treatment on numbers of total leukocytes (A), $CD4^+$ and $CD8^+$ T cell numbers (B), and B cell numbers (C) in peripheral blood, lungs, and spleens from ANDV-challenged and unchallenged hamsters on day 9 after ANDV challenge was determined by flow cytometry ($n = 3$). *P* values were determined by unpaired two-tailed Student's *t* test. NS, not significant. Values are means ± SDs. (D) The number of surviving hamsters for each group on each day after virus injection was determined ($n = 8$). The *P* value was determined by the log-rank survival test. Differences in survival were not significant.

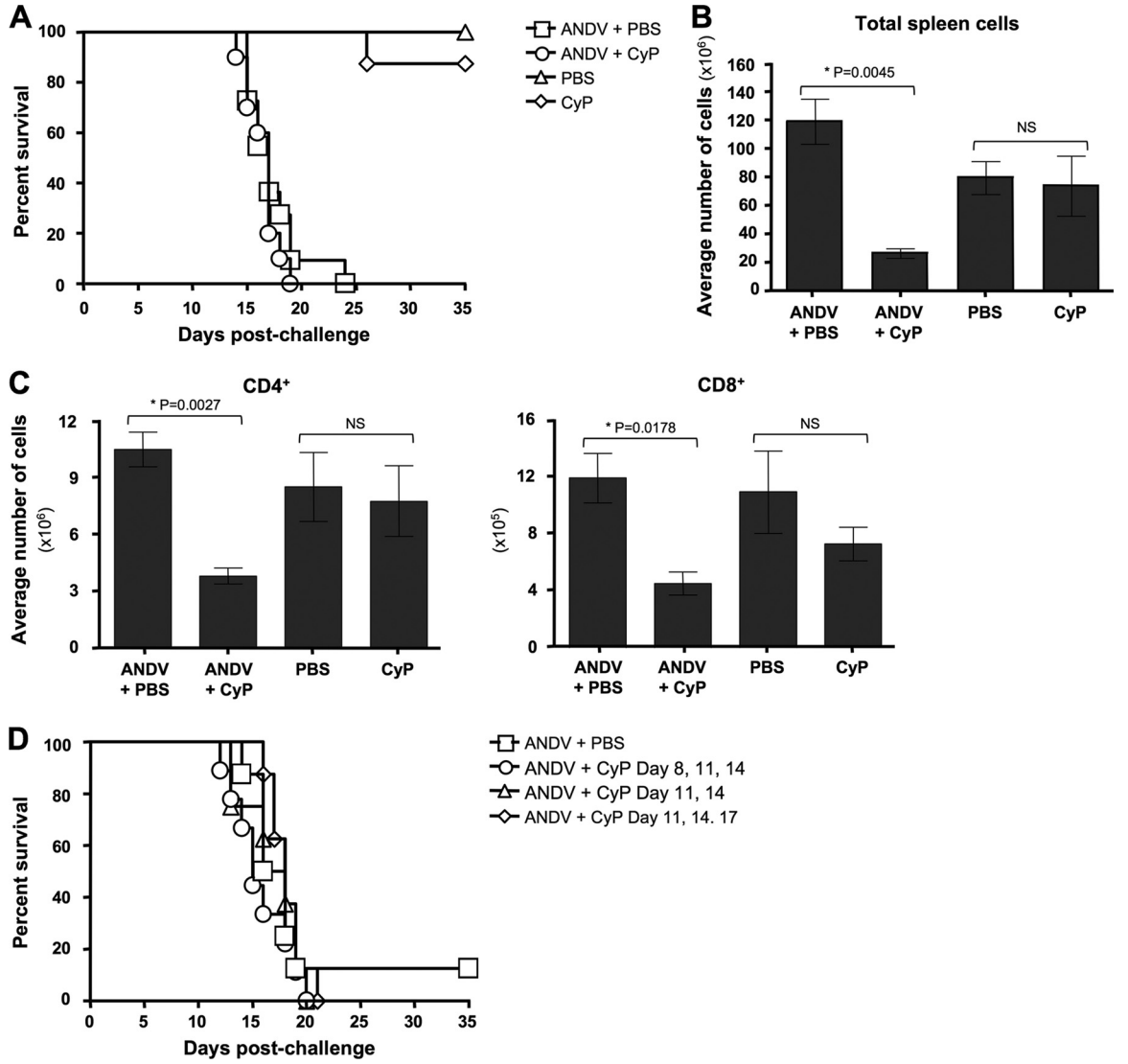

FIG. 4. Cyclophosphamide does not alter disease pathogenesis following intranasal ANDV challenge. Hamsters were challenged intranasally with 2,000 PFU of ANDV. At 8 and 11 days after challenge, hamsters challenged with ANDV were given 100 mg/kg cyclophosphamide intraperitoneally (ANDV + CyP) or an equivalent amount of PBS (ANDV + PBS). A separate group of hamsters that were not challenged with ANDV was given 100 mg/kg cyclophosphamide (CyP) or an equivalent amount of PBS. (A) The number of surviving hamsters for each group on each day after virus injection was determined ($n = 8$). The P value was determined by the log-rank survival test. Differences in survival were not significant. Spleens from ANDV-challenged and unchallenged hamsters receiving cyclophosphamide or PBS were harvested 15 days after ANDV challenge to determine the effects of cyclophosphamide treatment on total number of splenocytes (B) and the numbers of splenic $CD4^+$ and $CD8^+$ T cells ($n = 3$) (C). P values were determined by unpaired two-tailed Student's t test. NS, not significant. Values are means ± SDs. (D) In a second experiment, the number of surviving hamsters challenged with ANDV was determined after they were given PBS or 100 mg/kg cyclophosphamide intraperitoneally on days 8, 11, and 14; 11 and 14; or 11, 14, and 17 ($n = 8$). The P value was determined by the log-rank survival test. Differences in survival were not significant.

58, 69, 80, 85) or an altered course of disease (66). In response to intramuscular ANDV exposure, the accumulation of activated T cells peaks in the spleen and lung on day 9, a day before the onset of death (Fig. 2). This correlation suggested a role for T cells in pathogenesis. However, immunosuppression with CyP (Fig. 3 and 4) had no effect on the course of disease, either by increasing or by decreasing the time to death. CyP nonspecifically targets activated cells and might be expected to induce apoptosis of both pathogenic T cells and cell types necessary for protection. This could explain the lack of observable change in the time to death of infected animals. Nonetheless, specific depletion of T cells with antibody during the times when most T cell division occurred, 6 to 9 days postchallenge (Fig. 5), did not alter the course of disease either. To our knowledge, this is the first report of a study using immunodepletion to study mechanisms of T cell-mediated pathogenesis for any disease in the Syrian hamster. Most of the T cells recruited to the lung early after infection are likely not ANDV-specific T cells since T cell numbers tend to increase in the lung before measurable T cell division (Fig. 2). In much the

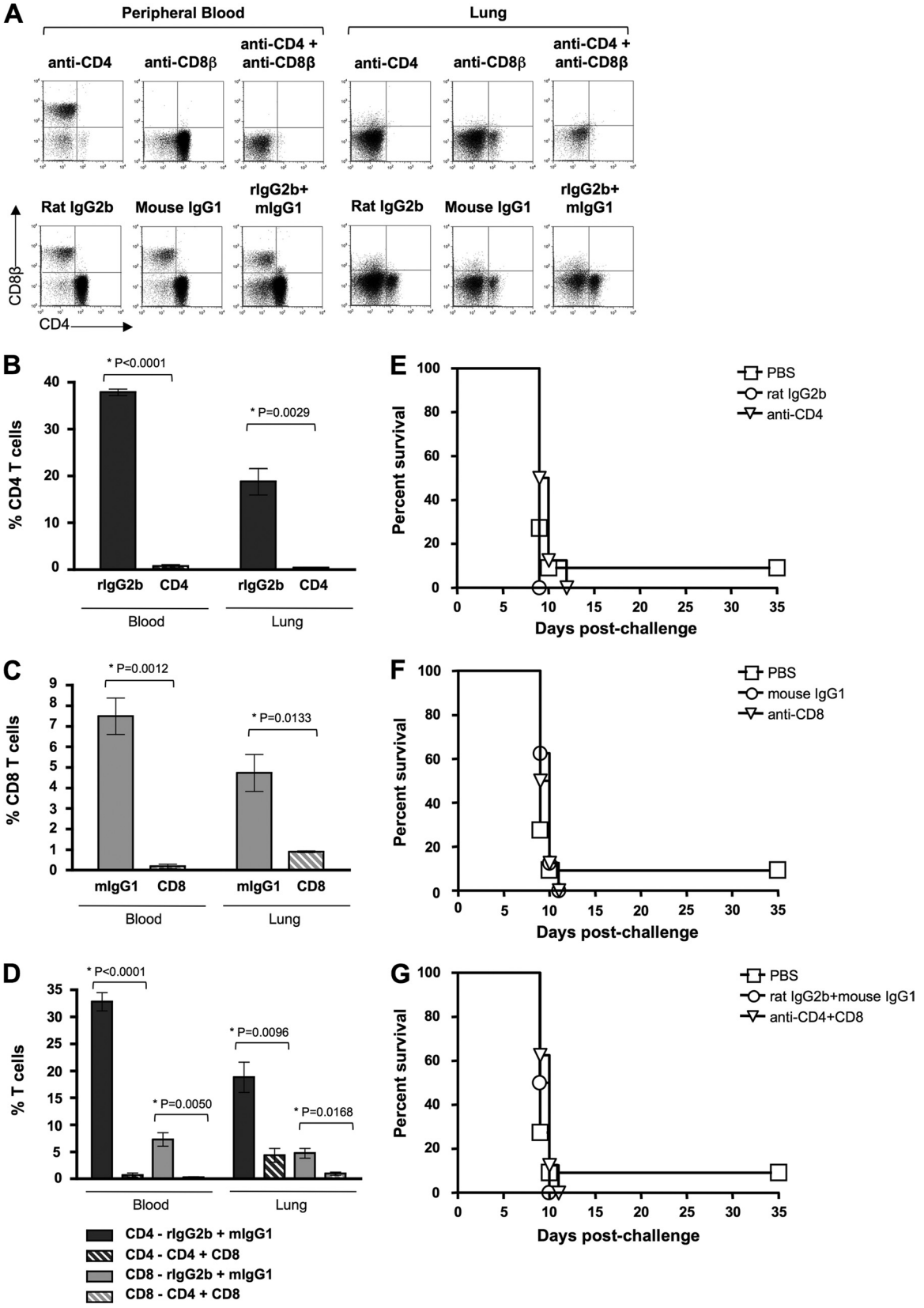
A
Peripheral Blood
Lung
anti-CD4
anti-CD8β
anti-CD4 + anti-CD8β
Rat IgG2b
Mouse IgG1
rIgG2b+ mIgG1
CD8β
CD4
B
% CD4 T cells
* P<0.0001
* P=0.0029
rIgG2b
CD4
Blood
Lung
C
% CD8 T cells
* P=0.0012
* P=0.0133
mIgG1
CD8
D
% T cells
* P<0.0001
* P=0.0050
* P=0.0096
* P=0.0168
CD4 - rIgG2b + mIgG1
CD4 - CD4 + CD8
CD8 - rIgG2b + mIgG1
CD8 - CD4 + CD8
E
Percent survival
Days post-challenge
PBS
rat IgG2b
anti-CD4
F
mouse IgG1
anti-CD8
G
rat IgG2b+mouse IgG1
anti-CD4+CD8

same way, memory T cells are nonspecifically recruited early to sites of infection (84). It is possible, though, that within this population of early T cell recruits exists a population of activated effector memory cells capable of cross-reacting with ANDV epitopes or activated naïve T cells (such as T_h2 cells) that have not undergone proliferation (3, 11, 43) but that may initiate a pathway to disease pathogenesis before being depleted. Nonetheless, given that the number of antigen-specific T cells ranges from 20 to 200 cells in an entire naïve animal (51), it seems unlikely that only a few hundred cells would be sufficient to cause disease. In agreement with this, when T cells were depleted beginning on day 4.5, no changes in the course of disease were observed. Thus, it seems that T cell accumulation in the lung merely correlates with disease but is not the cause of disease.

The vascular leak syndrome caused by ANDV infection of hamster shares many similarities with human HPS, including the incubation time, rapid disease onset, infected endothelial cells, pulmonary edema, pleural effusion, thrombocytopenia, neutrophilia, variability in heart rate, and hypotensive shock (8, 32, 83). Apparent discrepancies between the incubation time of HPS hantaviruses in hamsters and humans are largely due to the initial challenge dose and the route of exposure. Human HPS cases with well-defined exposures suggest a median incubation period of 14 to 18 days (82, 87). In hamsters, ANDV is lethal by multiple routes of exposure (31), but the time to disease onset can vary. Hamsters exposed to 2,000 PFU ANDV by i.m. injection have a mean time to death of 13 days, whereas hamsters exposed to 20 PFU by i.n. injection have a mean time to death of 25 days, well within the range expected for human cases. Interestingly, though, the numbers of viral genomes detected in the serum of humans and hamsters displaying clinical signs of HPS caused by SNV are remarkably similar (39, 83). Given that humans are likely exposed to significantly less virus than the hamsters used in these studies, the initial challenge dose may be irrelevant. Unfortunately, challenging hamsters with less than 80 PFU results in a more asynchronous disease course and large numbers of uninfected survivors, making results of analysis of immune response kinetics difficult to interpret.

$CD8^+$ T cells have been proposed to contribute to HPS in humans, and disease severity has been suggested to correlate with T cell number (39, 83). Nevertheless, changes in the size of the global T cell populations in the blood, spleen, and lungs of ANDV-infected hamsters (Fig. 2 and 3) appear to be smaller than what might be predicted from human HPS cases. It is likely, though, that the changes within the ANDV-specific T cell pool are more dramatic but are obscured by bulk analysis of the larger T cell population. In our studies, while it is not possible to identify ANDV-specific T cells on the basis of tetramer or intracellular cytokine staining due to a lack of hamster-specific reagents, changes in the number of $BrdU^+$ T cells (Fig. 2) (presumably ANDV specific) are more significant. Kilpatrick et al. (39) demonstrated that approximately 14% of $CD8^+$ T cells from humans suffering from severe to fatal HPS are specific for three different SNV epitopes. While it is likely that there are more than three ANDV $CD8^+$ T cell epitopes, the percentage of $BrdU^+$ $CD8^+$ T cells that we find 9 days after ANDV challenge is similar (Fig. 2). Alternatively, the fact that we demonstrate disease in the midst of a potentially less than overwhelming T cell response may be evidence against T cell-mediated immunopathology. Still, the correlation between $CD8^+$ T cell number and human HPS severity is tenuous. Most of the analysis of $CD8^+$ T cell responses during human HPS is limited to three viral epitopes presented by a single MHC I allele (39). Thus, the T cell responses to viral epitopes presented by other MHC I alleles are underrepresented, allowing for the possibility that total T cell responses during moderate and severe cases might be similar. The small sample size and the discontinuity in T cell numbers as disease severity increases also limit the strength of this correlation. Moreover, *in vitro* evidence that $CD8^+$ T cells obtained from an HFRS patient are able to specifically lyse endothelial cells expressing an SNV-derived peptide (29) does not accurately reflect the lack of endothelial cell apoptosis during human HPS. Since effector $CD8^+$ and $CD4^+$ T cells can secrete many of the same vasoactive cytokines, the $CD4^+$ subset in hamsters may be more likely to mediate pathogenesis in hamsters since it is more prevalent. Of these cytokines, tumor necrosis factor alpha (TNF-α) has been the most strongly linked with increased endothelial cell permeability. However, in two-thirds of fatal human HPS cases there was only a mild increase in the numbers of TNF-producing cells (52). Furthermore, recent evidence demonstrating that the hantavirus N protein can inhibit endothelial cell NK-κB activation induced by TNF-α (74) suggests a limited role for TNF-α in hantavirus pathogenesis. Nonetheless, depletion of neither subset ameliorated disease in hamsters (Fig. 5). We cannot exclude the possibility that HPS pathogenesis in humans is mechanistically different from that in hamsters or that hamsters do not reflect all the immunological changes during human HPS, but given the similarities in disease kinetics, presentation, and pathology between the two species, we believe that this is unlikely. As more reagents become available to study the Syrian hamster model, such as those recently identified by Zivcec et al. (89), identification of

FIG. 5. Depletion of T cells does not alter disease pathogenesis following intramuscular ANDV challenge. Hamsters were challenged intramuscularly with 2,000 PFU of ANDV. At 6 and 8 days after challenge, hamsters challenged with ANDV were given combinations of anti-CD4 and anti-CD8 antibodies, isotype control antibodies, or PBS i.p. (A) To confirm that T cells were depleted following the injection of antibody, peripheral blood and lung tissue from ANDV-challenged hamsters receiving antibody or PBS were analyzed by flow cytometry to determine the presence or absence of $CD4^+$ and $CD8^+$ subsets at 9 days postchallenge ($n = 3$). (B to G) The percentage of peripheral blood $CD4^+$ and $CD8^+$ T cells for each group was then determined, as was the number of surviving hamsters each day after virus challenge for groups receiving PBS, anti-CD4 antibody, or rat IgG2b isotype control antibody (B and E); PBS, anti-CD8 antibody, or mouse IgG1 isotype control antibody (C and F); or PBS, a combination of anti-CD4 and anti-CD8β antibodies, or rat IgG2b and mouse IgG1 isotype control antibodies (D and G) ($n = 8$). *P* values for T cell percentages were determined by unpaired two-tailed Student's *t* test. Values are means ± SDs. *P* values for survival were determined by the log-rank survival test. Differences in survival were not significant.

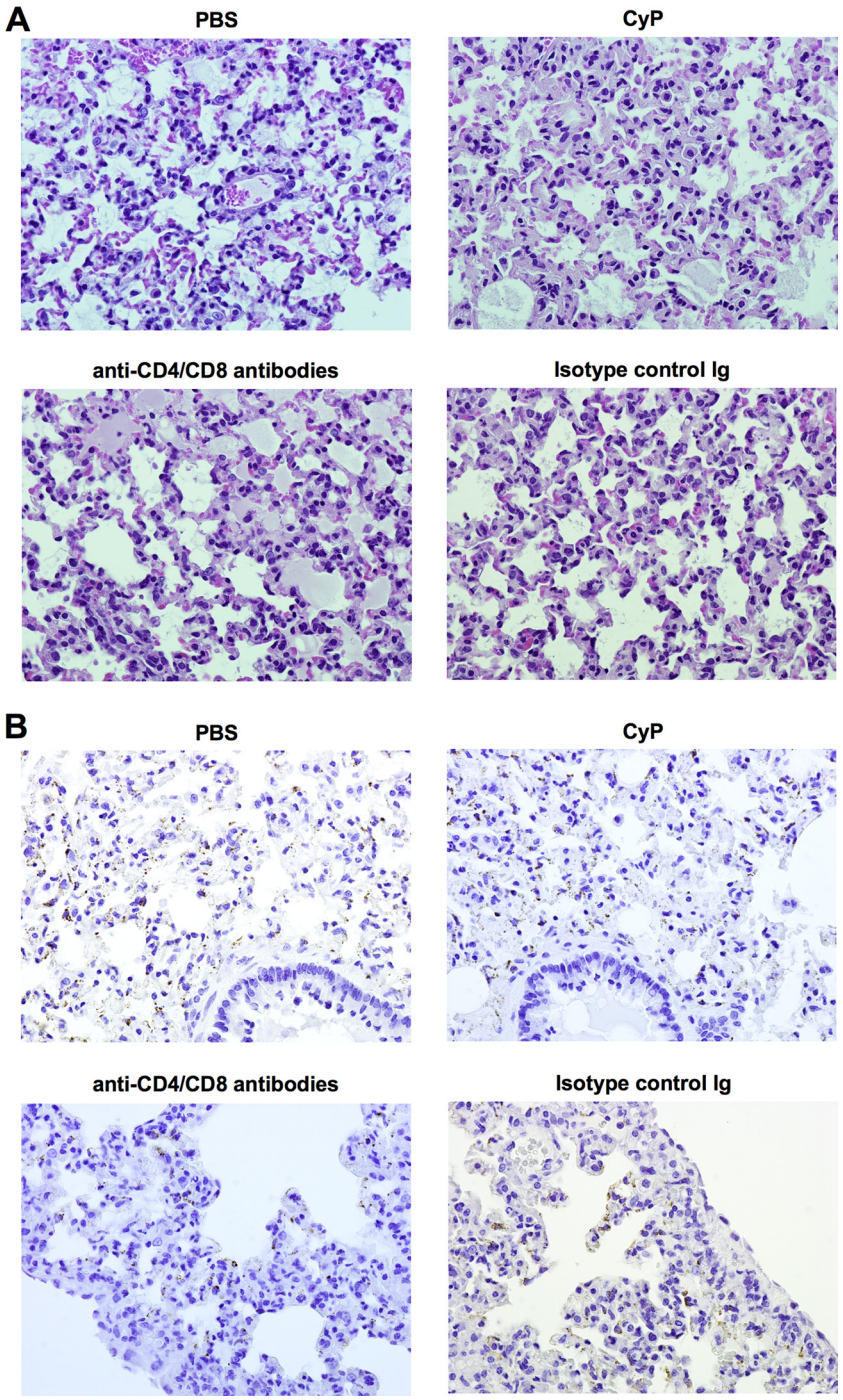

FIG. 6. Histomorphologic and immunohistochemistry analysis of lung tissue from hamsters challenged with ANDV. To determine if the depletion of T cells by CyP or antibody alters the pathogenesis of HPS in hamsters following a 2,000-PFU intramuscular ANDV infection, histomorphologic and immunohistochemistry analysis of lung tissue was performed 9 days after virus challenge. (A) Hematoxylin-eosin-stained lung tissue from ANDV-infected hamsters treated with PBS, CyP, CD4 and CD8 antibodies, or rat IgG2b plus mouse IgG1 isotype control antibodies was analyzed to identify any differences in gross ANDV pathology. (B) Immunohistochemical analysis of lung tissue was performed to determine any differences in the distribution of ANDV or viral load following treatment with PBS, CyP, CD4 and CD8 antibodies, or rat IgG2b plus mouse IgG1 isotype control antibodies. No differences were observed in gross pathology, viral distribution, or viral load between treatment groups.

any potential differences in HPS between hamsters and humans should become possible.

Many of the RNA viruses known to cause acute disease and pathology in humans do so by a combination of direct cytopathic effect and modulation of the expression of proinflammatory and vasoactive mediators, which lead to tissue damage and vascular permeability. Moreover, several viruses, including other hemorrhagic fever viruses, appear to share a mechanism

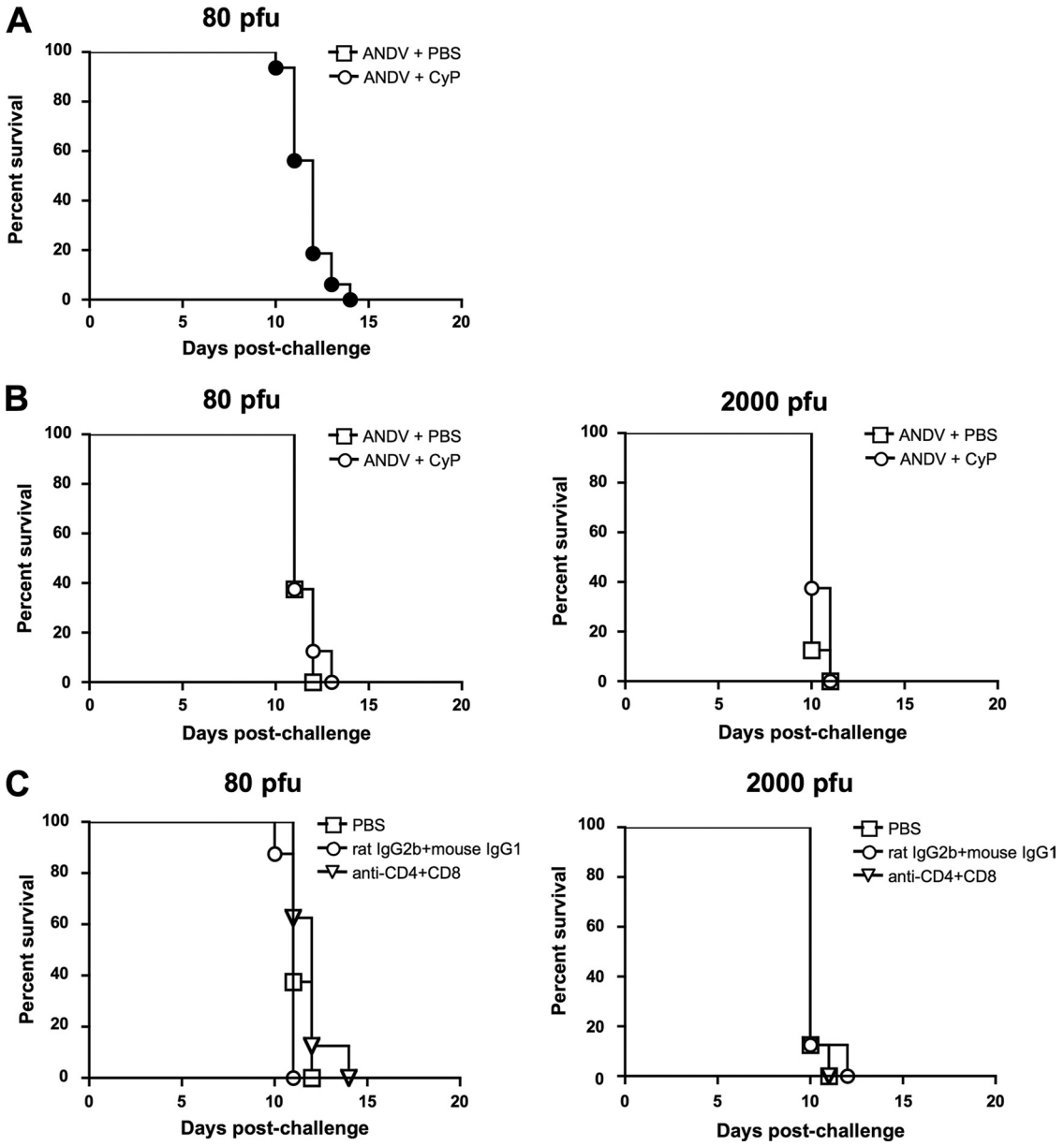

FIG. 7. Viral challenge dose and the timing of immunodepletion do not alter the course of hantavirus disease. (A) The kinetics of hantavirus disease in hamsters were determined following intramuscular challenge with 80 PFU of ANDV. (B) To determine if the challenge dose and the timing of CyP treatment would affect the ability of CyP to alter the course of hantavirus disease, hamsters were challenged with either 80 PFU ANDV (i.m.) or 2,000 PFU ANDV (i.m.). At 4, 6, and 8 days after challenge, hamsters were given 100 mg/kg cyclophosphamide intraperitoneally (ANDV + CyP) or an equivalent amount of PBS (ANDV + PBS). The number of surviving hamsters for each group on each day after virus injection was determined ($n = 8$). The P value was determined by the log-rank survival test. Differences in survival were not significant. (C) To determine if the challenge dose and the timing of T cell-depleting antibody treatment would affect the ability of T cell depletion to alter the course of hantavirus disease, hamsters were challenged with either 80 PFU ANDV (i.m.) or 2,000 PFU ANDV (i.m.). At 4, 6, and 8 days after challenge, hamsters were given PBS, a combination of anti-CD4 and anti-CD8β antibodies, or rat IgG2b and mouse IgG1 isotype control antibodies. The number of surviving hamsters for groups receiving PBS, a combination of anti-CD4 and anti-CD8β antibodies, or rat IgG2b and mouse IgG1 isotype control antibodies was determined each day after virus challenge ($n = 8$). The P value was determined by the log-rank survival test. Differences in survival were not significant.

of pathogenesis in which antigen-presenting cell types, macrophages, and dendritic cells (DCs) and not T cells are responsible for inducing vascular leakage. For example, influenza virus primarily targets alveolar epithelial cells, and pathology is likely mediated by a combination of direct cytopathic effect, dysregulated cytokine expression by neutrophils and macrophages, and macrophage-mediated epithelial cell apoptosis (30, 73, 78). Hemorrhagic fever viruses, such as Ebola viruses, dengue virus, and yellow fever virus, primarily target dendritic cells, macrophages, or tissue-specific cells such as hepatocytes (6, 24, 61, 65). While these viruses are directly cytopathic to many cell types, including endothelial cells, dysregulated ex-

pression of proinflammatory and vasoactive mediators by infected macrophages and activated NK cells has been implicated in perturbations in vascular integrity during primary infection (25, 62, 65). In this respect, hantaviruses are unique. Endothelial cells are the primary targets of hantaviruses, and infection of endothelial cells is noncytopathic. While primary human macrophages and dendritic cells are permissible to hantavirus infection *in vitro* (38, 48, 49), there is little evidence that these cell types or other immune cell types are primary targets during human infection. Hantavirus antigen has been detected in a small number of human macrophages during SNV infection of humans (52), but it is not clear if this is the result of direct infection or phagocytosed virus. *In vitro* infection of primary human macrophages and DCs by HPS-associated hantaviruses does result in the increased expression of HLA and costimulatory molecules associated with an activated phenotype (48, 49), although only ANDV infection of human monocyte-derived DCs resulted in a robust expression of soluble mediators (e.g., TNF-α and matrix metallopeptidase 9) capable of mediating vascular permeability and vascular remodeling (49). Alveolar macrophages are not immediately sensitive to CyP (34, 67), so our studies cannot exclude the possibility that proinflammatory and vasoactive mediators secreted by alveolar macrophages play a role in the vascular leakage associated with ANDV. Memory T cells have been implicated in dengue hemorrhagic fever caused by secondary dengue virus infection, but bystander T cell apoptosis effectively limits a role for T cells in protection or pathogenesis following Ebola virus infection. Little is known about the role, if any, that lymphocyte apoptosis during human HPS hantavirus infection might play in pathogenesis. Tuuminen et al. (79) and Akhmatova et al. (1) have demonstrated that T cells during the acute phase of infection with Puumala virus (HRFS) are more susceptible to apoptosis when stimulated than T cells during the convalescent phase. In these studies, though, it is not clear whether the T cells undergoing apoptosis are Puumala virus specific or T cells undergoing bystander apoptosis. The T cell apoptosis that we detect early after exposure to ANDV (Fig. 2) is likely bystander apoptosis of non-ANDV-specific T cells, given that ANDV antigen is not detectable in the blood or lung endothelial cells this early after ANDV infection (83). Jiang et al. (35) hypothesized that the early depletion of bystander T cells may allow space for the maximal expansion of antigen-specific T cells, but further experiments will need to be done to determine whether the early apoptosis of T cells following hantavirus infection enhances or impairs the ensuing T cell response.

The lack of effect of immune cell depletion in our studies, combined with the variability of immune responses even among fatal human HPS cases, would argue for a mechanism of pathogenesis in which hantavirus infection of endothelial cells directly results in dysfunction. One possible way that hantaviruses may directly interfere with endothelial cell function is by altering barrier function. The integrity of the vascular endothelium is maintained by a complex of tight junctions and adherens junctions. However, during vascular remodeling and wound repair, adherens junctions undergo a coordinated disassembly often controlled by vascular endothelial growth factor (VEGF). Adherens junctions are primarily composed of vascular endothelial (VE) cadherin (81) that interacts with and regulates VEGF signaling through the VEGF receptor (VEGFR) (19, 42). Similarly, VEGFR signaling is regulated by signaling cascades downstream of $\alpha_V\beta_3$ integrins (5, 64). Pathogenic hantaviruses bind to inactive β_3 integrin conformations on endothelial cells, causing them to remain inactive and interfering with their normal function (20, 22, 23, 63). Recently, this has been shown to result in dysregulation of VEGFR2 signaling, rendering infected endothelial cells hypersensitive to exogenous VEGF and increasing their permeability by altering the expression of genes that regulate endothelial cell migration and permeability and causing VE cadherin internalization, resulting in adherens junction disassembly (26, 27, 59). Notably, nonpathogenic hantaviruses infect endothelial cells via $\alpha_V\beta_1$ integrin, and this binding does not result in adherens junction disassembly. Subsequent studies have further demonstrated that *in vitro* ANDV infection of endothelial cells alone is sufficient to induce VEGF secretion, which occurs concurrently with VE cadherin internalization, and that, more importantly, serum from human HPS patients has increased levels of free VEGF (71). Whether the levels of VEGF in serum from human HPS patients correlate with disease severity and whether a similar mechanism is responsible for increased vascular permeability in hamsters infected with ANDV have yet to be elucidated. Still, such a mechanism would be expected to cause disease in a manner that is independent of the intensity of the immune response, although immune cells could conceivably contribute to increases in VEGF expression by expressing cytokines that induce VEGF expression (37). The observation that pathogenic hantaviruses also bind platelets and recruit them to the surface of endothelial cells via platelet-associated β_3 integrin, where they remain inactive (21), not only would explain the presence of platelet dysfunction (12) and thrombocytopenia during human and hamster hantavirus infection (12, 15, 40, 41, 57, 83, 88) but also would indicate how they contribute to the onset of hypoxia by virtue of how it may affect gas exchange within microcapillary beds. In this respect, a range of hypoxemia exists in HPS patients, and hyperoxygenation of HPS patients during extracorporeal membrane oxygenation (ECMO) therapy can reduce HPS mortality in severe cases (9, 13, 15, 28, 50). Hypoxia alone has been shown to induce VEGF expression (53, 60) by the induction of hypoxia-induced factor 1α (HIF1α) (46). This in turn may then augment the endothelial cell permeability already induced by VEGF secreted by infected endothelial cells.

HRFS and HPS continue to be neglected global health problems for which there are no FDA-licensed vaccines or effective postexposure prophylactics or therapeutics. Much of this can be attributed to a poor understanding of the mechanism of hantavirus pathogenesis. The reliance on correlations and circumstantial evidence has led to multiple proposed mechanisms, including T cell-mediated immunopathology. Nevertheless, by directly manipulating the Syrian hamster model, we can begin to elucidate or, at the very least, rule out potential mechanisms of disease. Here, for the first time, we demonstrated that HPS pathogenesis is not mediated by T cell, B cells, or other rapidly dividing immune cell types. While these studies reflect pathogenesis in the hamster model, this discovery should help to refocus efforts to understand hantavirus disease, which should in turn result in

effective therapeutic strategies to improve the outcome of human HPS.

ACKNOWLEDGMENTS

We thank M. Joselyn, L. Prugar, J. Moore, M. Winpigler, J. Fiallos, E. Blue, and W. Sifford for their excellent technical assistance. The mouse CD4, rat IgG2b, and mouse IgG1 antibodies were kindly purified by L. Altamura.

Opinions, interpretations, conclusions, and recommendations are ours and are not necessarily endorsed by the U.S. Army or the U.S. Department of Defense.

The experiments were designed by C.D.H. and J.W.H. C.D.H. performed the experimental work, and J.W.H. supervised the project. The manuscript was written by C.D.H. and J.W.H. Both authors approved the final manuscript.

REFERENCES

1. **Akhmatova, N. K., R. S. Yusupova, S. F. Khaiboullina, and S. V. Sibiryak.** 2003. Lymphocyte apoptosis during hemorrhagic fever with renal syndrome. Russ. J. Immunol. **8:**37–46.
2. **Alwan, W. H., F. M. Record, and P. J. Openshaw.** 1992. CD4+ T cells clear virus but augment disease in mice infected with respiratory syncytial virus. Comparison with the effects of CD8+ T cells. Clin. Exp. Immunol. **88:**527–536.
3. **Ben-Sasson, S. Z., R. Gerstel, J. Hu-Li, and W. E. Paul.** 2001. Cell division is not a "clock" measuring acquisition of competence to produce IFN-gamma or IL-4. J. Immunol. **166:**112–120.
4. **Borges, A. A., et al.** 2006. Hantavirus cardiopulmonary syndrome: immune response and pathogenesis. Microbes Infect. **8:**2324–2330.
5. **Borges, E., Y. Jan, and E. Ruoslahti.** 2000. Platelet-derived growth factor receptor beta and vascular endothelial growth factor receptor 2 bind to the beta 3 integrin through its extracellular domain. J. Biol. Chem. **275:**39867–39873.
6. **Bray, M.** 2005. Pathogenesis of viral hemorrhagic fever. Curr. Opin. Immunol. **17:**399–403.
7. **Brode, S., and A. Cooke.** 2008. Immune-potentiating effects of the chemotherapeutic drug cyclophosphamide. Crit. Rev. Immunol. **28:**109–126.
8. **Campen, M. J., M. L. Milazzo, C. F. Fulhorst, C. J. Obot Akata, and F. Koster.** 2006. Characterization of shock in a hamster model of hantavirus infection. Virology **356:**45–49.
9. **Chang, B., M. Crowley, M. Campen, and F. Koster.** 2007. Hantavirus cardiopulmonary syndrome. Semin. Respir. Crit. Care Med. **28:**193–200.
10. **Chen, L. B., and W. S. Yang.** 1990. Abnormalities of T cell immunoregulation in hemorrhagic fever with renal syndrome. J. Infect. Dis. **161:**1016–1019.
11. **Cook, K. D., and J. Miller.** TCR-dependent translational control of GATA-3 enhances Th2 differentiation. J. Immunol. **185:**3209–3216.
12. **Cosgriff, T. M., et al.** 1991. Platelet dysfunction contributes to the haemostatic defect in haemorrhagic fever with renal syndrome. Trans. R. Soc. Trop. Med. Hyg. **85:**660–663.
13. **Crowley, M. R., et al.** 1998. Successful treatment of adults with severe hantavirus pulmonary syndrome with extracorporeal membrane oxygenation. Crit. Care Med. **26:**409–414.
14. **Dondji, B., et al.** 2008. Role for nitric oxide in hookworm-associated immune suppression. Infect. Immun. **76:**2560–2567.
15. **Duchin, J. S., et al.** 1994. Hantavirus pulmonary syndrome: a clinical description of 17 patients with a newly recognized disease. The Hantavirus Study Group. N. Engl. J. Med. **330:**949–955.
16. **Easterbrook, J. D., and S. L. Klein.** 2008. Immunological mechanisms mediating hantavirus persistence in rodent reservoirs. PLoS Pathog. 4:e1000172.
17. **Ennis, F. A., et al.** 1997. Hantavirus pulmonary syndrome: CD8+ and CD4+ cytotoxic T lymphocytes to epitopes on Sin Nombre virus nucleocapsid protein isolated during acute illness. Virology **238:**380–390.
18. **Fulton, R. B., D. K. Meyerholz, and S. M. Varga.** Foxp3+ CD4 regulatory T cells limit pulmonary immunopathology by modulating the CD8 T cell response during respiratory syncytial virus infection. J. Immunol. **185:**2382–2392.
19. **Gavard, J., and J. S. Gutkind.** 2006. VEGF controls endothelial-cell permeability by promoting the beta-arrestin-dependent endocytosis of VE-cadherin. Nat. Cell Biol. **8:**1223–1234.
20. **Gavrilovskaya, I. N., E. J. Brown, M. H. Ginsberg, and E. R. Mackow.** 1999. Cellular entry of hantaviruses which cause hemorrhagic fever with renal syndrome is mediated by beta3 integrins. J. Virol. **73:**3951–3959.
21. **Gavrilovskaya, I. N., E. E. Gorbunova, and E. R. Mackow.** Pathogenic hantaviruses direct the adherence of quiescent platelets to infected endothelial cells. J. Virol. **84:**4832–4839.
22. **Gavrilovskaya, I. N., T. Peresleni, E. Geimonen, and E. R. Mackow.** 2002. Pathogenic hantaviruses selectively inhibit beta3 integrin directed endothelial cell migration. Arch. Virol. **147:**1913–1931.
23. **Gavrilovskaya, I. N., M. Shepley, R. Shaw, M. H. Ginsberg, and E. R. Mackow.** 1998. beta3 Integrins mediate the cellular entry of hantaviruses that cause respiratory failure. Proc. Natl. Acad. Sci. U. S. A. **95:**7074–7079.
24. **Geisbert, T. W., et al.** 2003. Pathogenesis of Ebola hemorrhagic fever in cynomolgus macaques: evidence that dendritic cells are early and sustained targets of infection. Am. J. Pathol. **163:**2347–2370.
25. **Geisbert, T. W., et al.** 2003. Mechanisms underlying coagulation abnormalities in Ebola hemorrhagic fever: overexpression of tissue factor in primate monocytes/macrophages is a key event. J. Infect. Dis. **188:**1618–1629.
26. **Gorbunova, E., I. N. Gavrilovskaya, and E. R. Mackow.** Pathogenic hantaviruses Andes virus and Hantaan virus induce adherens junction disassembly by directing vascular endothelial cadherin internalization in human endothelial cells. J. Virol. **84:**7405–7411.
27. **Gorbunova, E. E., I. N. Gavrilovskaya, T. Pepini, and E. R. Mackow.** VEGFR2 and Src kinase inhibitors suppress Andes virus-induced endothelial cell permeability. J. Virol. **85:**2296–2303.
28. **Hallin, G. W., et al.** 1996. Cardiopulmonary manifestations of hantavirus pulmonary syndrome. Crit. Care Med. **24:**252–258.
29. **Hayasaka, D., K. Maeda, F. A. Ennis, and M. Terajima.** 2007. Increased permeability of human endothelial cell line EA.hy926 induced by hantavirus-specific cytotoxic T lymphocytes. Virus Res. **123:**120–127.
30. **Herold, S., et al.** 2008. Lung epithelial apoptosis in influenza virus pneumonia: the role of macrophage-expressed TNF-related apoptosis-inducing ligand. J. Exp. Med. **205:**3065–3077.
31. **Hooper, J. W., A. M. Ferro, and V. Wahl-Jensen.** 2008. Immune serum produced by DNA vaccination protects hamsters against lethal respiratory challenge with Andes virus. J. Virol. **82:**1332–1338.
32. **Hooper, J. W., T. Larsen, D. M. Custer, and C. S. Schmaljohn.** 2001. A lethal disease model for hantavirus pulmonary syndrome. Virology **289:**6–14.
33. **Huang, C., B. Jin, M. Wang, E. Li, and C. Sun.** 1994. Hemorrhagic fever with renal syndrome: relationship between pathogenesis and cellular immunity. J. Infect. Dis. **169:**868–870.
34. **Hunninghake, G. W., and A. S. Fauci.** 1977. Immunological reactivity of the lung. IV. Effect of cyclophosphamide on alveolar macrophage cytotoxic effector function. Clin. Exp. Immunol. **27:**555–559.
35. **Jiang, J., L. L. Lau, and H. Shen.** 2003. Selective depletion of nonspecific T cells during the early stage of immune responses to infection. J. Immunol. **171:**4352–4358.
36. **Jonsson, C. B., L. T. Figueiredo, and O. Vapalahti.** 2010. A global perspective on hantavirus ecology, epidemiology, and disease. Clin. Microbiol. Rev. **23:**412–441.
37. **Jung, Y. J., J. S. Isaacs, S. Lee, J. Trepel, and L. Neckers.** 2003. IL-1beta-mediated up-regulation of HIF-1alpha via an NFkappaB/COX-2 pathway identifies HIF-1 as a critical link between inflammation and oncogenesis. FASEB J. **17:**2115–2117.
38. **Khaiboullina, S. F., D. M. Netski, P. Krumpe, and S. C. St Jeor.** 2000. Effects of tumor necrosis factor alpha on Sin Nombre virus infection in vitro. J. Virol. **74:**11966–11971.
39. **Kilpatrick, E. D., et al.** 2004. Role of specific CD8+ T cells in the severity of a fulminant zoonotic viral hemorrhagic fever, hantavirus pulmonary syndrome. J. Immunol. **172:**3297–3304.
40. **Koster, F., et al.** 2001. Rapid presumptive diagnosis of hantavirus cardiopulmonary syndrome by peripheral blood smear review. Am. J. Clin. Pathol. **116:**665–672.
41. **Lahdevirta, J.** 1982. Clinical features of HFRS in Scandinavia as compared with East Asia. Scand. J. Infect. Dis. Suppl. **36:**93–95.
42. **Lampugnani, M. G., F. Orsenigo, M. C. Gagliani, C. Tacchetti, and E. Dejana.** 2006. Vascular endothelial cadherin controls VEGFR-2 internalization and signaling from intracellular compartments. J. Cell Biol. **174:**593–604.
43. **Lanzavecchia, A., and F. Sallusto.** 2005. Understanding the generation and function of memory T cell subsets. Curr. Opin. Immunol. **17:**326–332.
44. **Lazaro, M. E., et al.** 2007. Clusters of hantavirus infection, southern Argentina. Emerg. Infect. Dis. **13:**104–110.
45. **Liu, H., B. M. Steiner, J. D. Alder, D. K. Baertschy, and R. F. Schell.** 1990. Immune T cells sorted by flow cytometry confer protection against infection with Treponema pallidum subsp. pertenue in hamsters. Infect. Immun. **58:**1685–1690.
46. **Liu, L. X., et al.** 2002. Stabilization of vascular endothelial growth factor mRNA by hypoxia-inducible factor 1. Biochem. Biophys. Res. Commun. **291:**908–914.
47. **Makela, S., et al.** 2002. Human leukocyte antigen-B8-DR3 is a more important risk factor for severe Puumala hantavirus infection than the tumor necrosis factor-alpha(-308) G/A polymorphism. J. Infect. Dis. **186:**843–846.
48. **Markotic, A., et al.** 2007. Pathogenic hantaviruses elicit different immunoreactions in THP-1 cells and primary monocytes and induce differentiation of human monocytes to dendritic-like cells. Coll. Antropol. **31:**1159–1167.
49. **Marsac, D., et al.** Infection of human monocyte-derived dendritic cells by Andes hantavirus enhances pro-inflammatory state, the secretion of active MMP-9 and indirectly enhances endothelial permeability. Virol. J. **8:**223.
50. **Mertz, G. J., et al.** 2006. Diagnosis and treatment of New World hantavirus infections. Curr. Opin. Infect. Dis. **19:**437–442.

51. **Moon, J. J., et al.** 2007. Naive CD4(+) T cell frequency varies for different epitopes and predicts repertoire diversity and response magnitude. Immunity **27:**203–213.
52. **Mori, M., et al.** 1999. High levels of cytokine-producing cells in the lung tissues of patients with fatal hantavirus pulmonary syndrome. J. Infect. Dis. **179:**295–302.
53. **Mukhopadhyay, D., et al.** 1995. Hypoxic induction of human vascular endothelial growth factor expression through c-Src activation. Nature **375:**577–581.
54. **Mustonen, J., et al.** 1994. Renal biopsy findings and clinicopathologic correlations in nephropathia epidemica. Clin. Nephrol. **41:**121–126.
55. **Mustonen, J., et al.** 1998. Association of HLA B27 with benign clinical course of nephropathia epidemica caused by Puumala hantavirus. Scand. J. Immunol. **47:**277–279.
56. **Mustonen, J., et al.** 1996. Genetic susceptibility to severe course of nephropathia epidemica caused by Puumala hantavirus. Kidney Int. **49:**217–221.

56a. **National Research Council.** 1996. Guide for the care and use of laboratory animals. National Academy Press, Washington, DC.

57. **Nolte, K. B., et al.** 1995. Hantavirus pulmonary syndrome in the United States: a pathological description of a disease caused by a new agent. Hum. Pathol. **26:**110–120.
58. **Ostler, T., W. Davidson, and S. Ehl.** 2002. Virus clearance and immunopathology by CD8(+) T cells during infection with respiratory syncytial virus are mediated by IFN-gamma. Eur. J. Immunol. **32:**2117–2123.
59. **Pepini, T., E. E. Gorbunova, I. N. Gavrilovskaya, J. E. Mackow, and E. R. Mackow.** 2010. Andes virus regulation of cellular microRNAs contributes to hantavirus-induced endothelial cell permeability. J. Virol. **84:**11929–11936.
60. **Pham, I., et al.** 2002. Hypoxia upregulates VEGF expression in alveolar epithelial cells in vitro and in vivo. Am. J. Physiol. Lung Cell. Mol. Physiol. **283:**L1133–L1142.
61. **Quaresma, J. A., et al.** 2007. Hepatocyte lesions and cellular immune response in yellow fever infection. Trans. R. Soc. Trop. Med. Hyg. **101:**161–168.
62. **Quaresma, J. A., et al.** 2006. Revisiting the liver in human yellow fever: virus-induced apoptosis in hepatocytes associated with TGF-beta, TNF-alpha and NK cells activity. Virology **345:**22–30.
63. **Raymond, T., E. Gorbunova, I. N. Gavrilovskaya, and E. R. Mackow.** 2005. Pathogenic hantaviruses bind plexin-semaphorin-integrin domains present at the apex of inactive, bent alphavbeta3 integrin conformers. Proc. Natl. Acad. Sci. U. S. A. **102:**1163–1168.
64. **Robinson, S. D., L. E. Reynolds, L. Wyder, D. J. Hicklin, and K. M. Hodivala-Dilke.** 2004. Beta3-integrin regulates vascular endothelial growth factor-A-dependent permeability. Arterioscler. Thromb. Vasc. Biol. **24:**2108–2114.
65. **Rodenhuis-Zybert, I. A., J. Wilschut, and J. M. Smit.** 2010. Dengue virus life cycle: viral and host factors modulating infectivity. Cell. Mol. Life Sci. **67:**2773–2786.
66. **Ruzek, D., et al.** 2009. CD8+ T-cells mediate immunopathology in tick-borne encephalitis. Virology **384:**1–6.
67. **Santosuosso, M., M. Divangahi, A. Zganiacz, and Z. Xing.** 2002. Reduced tissue macrophage population in the lung by anticancer agent cyclophosphamide: restoration by local granulocyte macrophage-colony-stimulating factor gene transfer. Blood **99:**1246–1252.
68. **Schmaljohn, C. S., and J. W. Hooper.** 2001. Bunyaviridae: the viruses and their replication, p. 1581–1602. *In* D. M. Knipe et al. (ed.), Fields virology, 4th ed. Lippincott Williams and Wilkins, Philadelphia, PA.
69. **Schwarze, J., et al.** 1999. CD8 T cells are essential in the development of respiratory syncytial virus-induced lung eosinophilia and airway hyperresponsiveness. J. Immunol. **162:**4207–4211.
70. **Shrestha, B., and M. S. Diamond.** 2004. Role of CD8+ T cells in control of West Nile virus infection. J. Virol. **78:**8312–8321.
71. **Shrivastava-Ranjan, P., P. E. Rollin, and C. F. Spiropoulou.** 2010. Andes virus disrupts the endothelial cell barrier by induction of vascular endothelial growth factor and downregulation of VE-cadherin. J. Virol. **84:**11227–11234.
72. **Sun, J., R. Madan, C. L. Karp, and T. J. Braciale.** 2009. Effector T cells control lung inflammation during acute influenza virus infection by producing IL-10. Nat. Med. **15:**277–284.
73. **Taubenberger, J. K., and D. M. Morens.** 2008. The pathology of influenza virus infections. Annu. Rev. Pathol. **3:**499–522.
74. **Taylor, S. L., R. L. Krempel, and C. S. Schmaljohn.** 2009. Inhibition of TNF-alpha-induced activation of NF-kappaB by hantavirus nucleocapsid proteins. Ann. N. Y. Acad. Sci. **1171**(Suppl. 1)**:**E86–E93.
75. **Temonen, M., et al.** 1996. Cytokines, adhesion molecules, and cellular infiltration in nephropathia epidemica kidneys: an immunohistochemical study. Clin. Immunol. Immunopathol. **78:**47–55.
76. **Terajima, M., D. Hayasaka, K. Maeda, and F. A. Ennis.** 2007. Immunopathogenesis of hantavirus pulmonary syndrome and hemorrhagic fever with renal syndrome: do CD8+ T cells trigger capillary leakage in viral hemorrhagic fevers? Immunol. Lett. **113:**117–120.
77. **Toro, J., et al.** 1998. An outbreak of hantavirus pulmonary syndrome, Chile, 1997. Emerg. Infect. Dis. **4:**687–694.
78. **Tumpey, T. M., et al.** 2005. Pathogenicity of influenza viruses with genes from the 1918 pandemic virus: functional roles of alveolar macrophages and neutrophils in limiting virus replication and mortality in mice. J. Virol. **79:**14933–14944.
79. **Tuuminen, T., et al.** 2007. Human CD8+ T cell memory generation in Puumala hantavirus infection occurs after the acute phase and is associated with boosting of EBV-specific CD8+ memory T cells. J. Immunol. **179:**1988–1995.
80. **Varga, S. M., X. Wang, R. M. Welsh, and T. J. Braciale.** 2001. Immunopathology in RSV infection is mediated by a discrete oligoclonal subset of antigen-specific CD4(+) T cells. Immunity **15:**637–646.
81. **Venkiteswaran, K., et al.** 2002. Regulation of endothelial barrier function and growth by VE-cadherin, plakoglobin, and beta-catenin. Am. J. Physiol. Cell Physiol. **283:**C811–C821.
82. **Vial, P. A., et al.** 2006. Incubation period of hantavirus cardiopulmonary syndrome. Emerg. Infect. Dis. **12:**1271–1273.
83. **Wahl-Jensen, V., et al.** 2007. Temporal analysis of Andes virus and Sin Nombre virus infections of Syrian hamsters. J. Virol. **81:**7449–7462.
84. **Wakim, L. M., T. Gebhardt, W. R. Heath, and F. R. Carbone.** 2008. Cutting edge: local recall responses by memory T cells newly recruited to peripheral nonlymphoid tissues. J. Immunol. **181:**5837–5841.
85. **Xu, L., et al.** 2004. Cutting edge: pulmonary immunopathology mediated by antigen-specific expression of TNF-alpha by antiviral CD8+ T cells. J. Immunol. **173:**721–725.
86. **Yanagihara, R., and D. J. Silverman.** 1990. Experimental infection of human vascular endothelial cells by pathogenic and nonpathogenic hantaviruses. Arch. Virol. **111:**281–286.
87. **Young, J. C., et al.** 2000. The incubation period of hantavirus pulmonary syndrome. Am. J. Trop. Med. Hyg. **62:**714–717.
88. **Zaki, S. R., et al.** 1995. Hantavirus pulmonary syndrome. Pathogenesis of an emerging infectious disease. Am. J. Pathol. **146:**552–579.
89. **Zivcec, M., D. Safronetz, E. Haddock, H. Feldmann, and H. Ebihara.** 2011. Validation of assays to monitor immune responses in the Syrian Golden hamster (Mesocricetus auratus). J. Immunol. Methods **368:**24–35.